Deglycerolization of Biodiesel Streams by Adsorption Over Silica Beds

J. C. Yori, S. A. D'Ippolito, C. L. Pieck, and C. R. Vera*

Instituto de Investigaciones en Catálisis y Petroquímica, INCAPE (FIQ-UNL, CONICET), Santiago del Estero 2654, 3000 Santa Fe, Argentina

Received August 6, 2006. Revised Manuscript Received September 13, 2006

A simple method for the almost complete removal of glycerol from methanol-free biodiesel streams coming out from industrial transesterification reactors is presented. The method is posed as a "dry" alternative to the conventional "wet" methods involving water washing. It is based on the use of silica beds and relies on the adsorption at room temperature to retain the small amounts of glycerol dissolved in the solutions of fatty acid methyl esters and adjust their content to the quality standards for biodiesel fuel. Fresh silica has a great processing capacity and the breakthrough of the bed depends mainly on the feed rate, the concentration of glycerol, and the mass of adsorbent. In the case of the silica gel used, the saturation capacity was found to be 0.13 g of glycerol per gram of silica. If the particle diameter is 1−1.5 mm, the breakthrough and saturation point almost coincide and the full capacity of the bed is used. However, industrial adsorption units with $^1/_8$ in. silica beads suffer from mass-transfer limitations inside the pellet pores, and for this particle size, the breakthrough point ($C/C^0 = 0.01$) is located at about one-half of the time of full saturation. For a glycerol concentration of 0.11−0.25% typical of biodiesel streams issuing from gravity settling tanks and an entrance velocity of 11 cm min^{-1}, a 2 m high silica bed with $^1/_8$ in. beads has a breakthrough point of 8 h and a net processing capacity of 0.01−0.02 $m^3_{biodiesel}$ kg_{silica}^{-1}. The breakthrough curves were studied using approximate solutions to the set of differential equations. Assuming a linear isotherm gives erroneous results; fitting the experimental breakthrough curves produces underestimated values of the Henry's adsorption constant and of the mass-transfer resistances. Modeling the high dilution regime with the UNIFAC method gives more realistic values of the Henry's constant (1.1 m^3 kg^{-1}). The experimentally measured saturation capacity is close to the monolayer capacity (13−15% w/w). These values give a Langmuir isotherm which can be fairly well approximated by a square irreversible isotherm. Accordingly, breakthrough curves were fairly well predicted using an irreversible isotherm, a shrinking-core adsorption model, and common correlations for the mass-transfer coefficients. The silica bed was succesfully regenerated eluting 4 bed volumes of methanol and drying in a nitrogen stream for 1 h. Temperature programmed oxidation tests of fresh, regenerated, and glycerol impregnated silica pellets indicated that desorption of glycerol was practically complete. In the industrial practice, the eluted volume can be recycled to the transesterification reactors with no waste of products or reactants. Evaporation of the adsorbed methanol during drying of the bed produced a decrease of the bed temperature and about 200 kJ kg_{silica}^{-1} should be provided in order to maintain the temperature.

Introduction

Biodiesel is a diesel fuel substitute produced by the transesterification of fatty substances like oils and fats. Lately, its production and its use have increased in many countries and are in nascent status in many others. Biodiesel is nowadays technically competitive with petrodiesel and requires practically no changes in the fuel distribution system. Some other advantages of biodiesel compared to petroleum-derived diesel include reduction of most tailpipe emissions, higher lubricity and flash point, biodegradability, and domestic origin.[1]

Currently, three common types of biodiesel production technologies are available, and the selection of any of them depends mainly on feedstock quality.[2] Methyl esters are produced from fats and oils, which are composed of triglycerides. Feedstocks that contain free fatty acids can be used for producing biodiesel but require different conversion processes. The commercially used processes for biodiesel production are the following: (i) base-catalyzed transesterification with refined oils; (ii) base-catalyzed transesterification with low free fatty acid greases and fats; (iii) acid esterification followed by transesterification of low or high free fatty acid greases and fats. Each of these processes typically utilizes methanol in the presence of a base catalyst such as NaOH or KOH to produce a monoester-based oxygenated fuel and glycerol as a byproduct.

Removal of glycerol and glycerides from biodiesel is an important step of the process because key aspects of the quality of the fuel strongly depend on the content of free and bound glycerol. The ASTM D6751 and EN 14214 standards establish a maximum amount of 0.02% of free glycerin and 0.24−0.25% total glycerol (free and bound). When heated, glycerol tends to polymerize by condensation with other molecules of glycerol or glycerides. Glycerides also increase the cloud point of biodiesel by forming small crystals at low temperatures. The equilibrium glycerol content in biodiesel issuing from a decanter depends strongly on the residual methanol content of the stream which acts as a cosolvent. When methanol is completely

* Corresponding author. E-mail: cvera@fiqus.unl.edu.ar. Tel.: +54-342-4533858. Fax: +54-342-4531068.

(1) Srivastava, A.; Prasad, R. *Renewable Sustainable Energy Rev.* **2000**, *4*, 111.

(2) Mittelbach, M.; Roncar, M. Method for the preparation of fatty acid alkyl esters. US Patent 5,849,939, 1998.

10.1021/ef060362d CCC: $37.00
Published on Web 11/24/2006

removed, the free glycerin content depends only on the temperature. According to Kimmel[3] and Negi,[4] it is approximately 0.2% at 25 °C and increases linearly as a function of the temperature. Even if methanol is not present, hydrophilic glycerol can be solubilized in the oily phase by the mediation of monoglycerides (MG) and diglycerides (DG) serving as amphiphilic substances. DG and MG can be separated from the oil and precipitated as a result of changes in storage time and temperature. This phenomenon reduces also the solubilization degree of glycerol in oil and produces the separation and precipitation of glycerol. If this occurs in the pipes of the car fuel system, many problems can arise. Glycerol in the motor also glazes cylinders, gums up rings, and causes injector coking

Glycerol removal is customarily performed in the industrial practice by washing with water. This method uses the high affinity between glycerol and water; the standard molar enthalpy of hydration of glycerol is -103.47 kJ mol^{-1}. The water-washing step is primarily aimed at removing the small amounts of glycerol and alkaline substances contained in biodiesel. Another purpose is to remove amphiphilic substances such as DG and MG, through partition-dissolution in water. Theoretically speaking, if water-washing is used to remove glycerin and a comparative amount of dissolved alkaline substance in the absence of glycerides, large amounts of water should not be required. However in the presence of MG and DG, addition of a small amount of water to the oil phase results in the formation of an emulsion upon stirring. Particularly when this operation is performed at a low-temperature, separation of the aqueous phase from the emulsion becomes difficult. Typically, the emulsion must be left to stand for long times in order to form a two-layer system or must be centrifuged. In order to prevent the formation of such an emulsion in the conventional water-washing practice, a large amount of water must be used. These large amounts of water usually need to be separated from the oil phase by centrifugation stages.

The amount of wastewater in conventional biodiesel production processes has not yet been an issue, but things may change due to environmental concerns. Currently, the water consumption is larger than 3 g of water per gram of biodiesel. Karaosmanoglu et al.[5] investigated the refining step of biodiesel and concluded that a minimum of 3−5 g of water per gram of biodiesel at 50 °C is needed to efficiently remove the impurities of the fuel. The reduction of the wastewater of biodiesel production is specially important in small facilities that cannot afford the setup of wastewater units. Some reports in this direction have lately appeared. Nakayama and Tsuto[6] used a combination of limited washing and a high-water-absorptive resin to remove the impurities of biodiesel. Özgül and Turkay[7] have proposed to use the adsorption of biodiesel impurities over rice hulls. Bournay et al.[8] recently reported a heterogeneous biodiesel production process that uses an adsorber for removing soluble glycerol.

The use of fixed beds of silica gel for the adsorption of glycerol contained in methanol-free biodiesel streams was studied in this work. Experimental and reported data on the adsorption of glycerol over some adsorbents, thermodynamic formulas, and differential mass balance equations were used to model glycerol bed adsorbers. The results were compared against breakthrough curves obtained experimentally.

Experimental

Materials. Methyl soyate was prepared according to a method described elsewhere.[9] Biodiesel was further purified from glycerol and glycerides by repeated cycles of washing with distilled water and centrifugation, until the glycerol concentration was lower than 0.005% by gas chromatography analysis. Biodiesel was also methanol-free by GC. Biodiesel:glycerol solutions were prepared using this biodiesel and pure glycerol. Pure glycerol was supplied by Sintorgan (>99.5%). For gas chromatography (GC) analysis calibration, a stock solution of glycerol (1.21 g L^{-1}) was prepared.

Gas Chromatography Analysis. The method of Plank and Lorbeer[10] was used because it was the adopted in the ASTM and EN norms for measuring glycerides and glycerol in biodiesel. First, stock solutions of two internal standards were prepared using pyridine (Merck, 99.9%) as solvent: a 1,2,4-butanetriol (Assay, >95%, GC), Fluka stock solution (4.07 g L^{-1}), and a tricaprin (Fluka, > 99%) stock solution (10 g L^{-1}). The samples to be analyzed were prepared in the following fashion: 70 μL of the butanetriol stock solution and 100 μL of the tricaprin stock solution were added as internal standards to 100−110 mg of the sample to be analyzed in a 10 mL screw-cap vial. Then, 100 μL of MSTFA (Aldrich) were added to the vial. After 15 min at room temperature, the silylated mixtures were dissolved in *n*-heptane (Merck, 99.5+%) and diluted to 5 mL. To aid the identification of MG, a standard of myristin (>99%, Fluka) was used (1 g L^{-1}).

The analyses were performed with a Varian Star 3400 CX gas chromatograph equipped with an on-column Supelco injector and a flame-ionization detector (FID). The column was a Zebron ZB-5 (Phenomenex), 25 m × 0.25 mm i.d. fused-silica capillary column. The samples were injected manually at an oven temperature of 50 °C. After an isothermal period of 1 min, the chromatograph oven was heated at 15 °C min^{-1} to 180 °C, at 7 °C min^{-1} to 230 °C, and ballistically to 300 °C (held for 20 min). Nitrogen was used as a carrier gas at a flow rate of 3 mL min^{-1}. The detector temperature was 350 °C; nitrogen served as the detector make up gas at an inlet pressure of 0.5 bar. The total run time was 90 min.

Glycerol Breakthrough Curves. A stainless steel tube of 0.25 in. internal diameter and 30 cm length was loaded with white silica gel (Grace Davison Co., Sg = 280 m^2 g^{-1}) crushed and sieved to 10−40 meshes (final bulk density = 0.54 g mL^{-1}). In a typical experiment, a biodiesel:glycerol solution (0.1−0.2% glycerol) was injected over a fresh charge of adsorbent at a space velocity of 3−11 cm min^{-1}, a velocity common of solid−liquid adsorption systems.[11] Flushing with methanol (Dorwil, 99.9%) at the same space velocity and drying with nitrogen (AGA, water-free, 150 mL min^{-1}, 1 h) was performed to regenerate the bed.

Results and Discussion

Linear Isotherm Model. For modeling the adsorption of glycerol over the adsorbent bed, several simplyfing assumptions were made: (i) The whole system was considered to be isothermal. (ii) The flow pattern was supposed to be that of the axially dispersed Fickian flow; radial concentration and temperature gradients in the adsorption bed were considered negligible. (iii) The adsorption of glycerol was considered to follow Henry's law (high dilution regime, second term of eq 4). (iv) The axial diffusion D_L and the film coefficient k_f were supposed to obey the Wakao and Funazkri correlations

(3) Kimmel, T. Kinetic investigation of the base-catalyzed glycerolysis of fatty acid methyl esters. Doctoral Thesis, Institut für Chemie, Technischen Universität Berlin, Berlin, Germany, 2004.

(4) Negi, D. S.; Sobotka, F.; Kimmel, T.; Wozny, G.; Schomäcker, R. *Ind. Eng. Chem. Res.* **2006**, *45*, 3693.

(5) Karaosmanoglu, F.; Cigizoglu, K. B.; Tuter, M.; Ertekin, S. *Energy Fuels* **1996**, *10*, 890.

(6) Nakayama, M.; Tsuto, K. Method of producing fatty acid alkyl ester for diesel fuel oil. European Patent EP 1,477,549, 2004.

(7) Özgül-Yücel, S.; Turkay, S. *JAOCS* **2001**, *80*, 373.

(8) Bournay, L.; Casanave, D.; Delfort, B.; Hillion, G.; Chodorge, J.A. *Catal. Today* **2005**, *106*, 190.

(9) Noureddini, H.; Zhu, D. *JAOCS* **1997**, *74*, 1457.

(10) Plank, C.; Lorbeer, E. *J. Chromatogr., A* **1995**, *697*, 461.

(11) Teo, W. K.; Ruthven, D. M. *Ind. Eng. Chem. Process Des. Dev.* **1986**, *25*, 17.

(2−3).[12] (v) The transfer through the film of the pellet was described by a classical linear relation (5). Applying these assumptions to a mass balance through a packed bed, eqs 1−9 were obtained. The explanation of the meaning of each symbol is given in Table 1.

$$\frac{\partial C}{\partial t} - D_L \frac{\partial^2 C}{\partial z^2} + \frac{\partial (uC)}{\partial z} + \frac{1-\epsilon}{\epsilon}\rho_p \frac{\partial q}{\partial t} = 0 \quad (1)$$

$$\frac{D_L}{2uR_p} = \frac{20}{ReSc} + 0.5 \quad (2)$$

$$k_f = (2.0 + 1.1Sc^{1/3}Re^{0.6})\frac{D_m}{2R_p} \quad (3)$$

$$q^* = \frac{q_m K_L C}{1 + K_L C} \approx KC \quad (4)$$

$$\frac{\partial q}{\partial t} = (3k_f/(R_p\rho_p))(C - q_s/K) \quad (5)$$

$$C(0,t) = C^0 \quad (6)$$

$$\frac{\partial C}{\partial z} = 0, \quad z = L \quad (7)$$

$$C(z,0) = 0 \quad (8)$$

Equations (6−8) are the "clean bed" initial condition and the Danckwertz boundary conditions for a closed system. The previous system is incomplete without a description of the mass flux inside the pellet. In the most common form, this is the equation of diffusion inside a spherical pellet.

$$\frac{\partial q}{\partial t} = D_p\left(\frac{\partial^2 q}{\partial r^2} + \frac{2}{r}\frac{\partial q}{\partial r}\right) \quad (9)$$

The solution to the previous system is presented in Figure 1. The whole $C-z-t$ set of solutions for arbitrary z and initial C^0 were obtained using the Q-LND (quasi-log normal) approximation in the form described by Li et al.[13] The value of each parameter of eqs 1−9 is given in Table 1. Experimental values of the breakthrough curve are also plotted that correspond to a test for $U = 11$ cm min^{-1}. In order to see the influence of transport parameters, additional theoretical solutions were obtained by decreasing the axial diffusivity or increasing the film mass-transfer coefficient by a factor of 100. The effect of the axial diffusion was negligible in determining the sigmoidal shape of the curve. Only the value of k_f seems to explain the smoother variation of the theoretical model with respect to the experimental one. D_M was calculated using the Wilke−Chang equation, and practically the same value reported elsewhere was obtained.[3] When increasing the k_f value from that calculated using the Wakao−Funazkri correlation, the shape of the breakthrough curve becomes more similar to that of the experimental curve. It is known that Wakao−Funazkri correlations are only valid for $Re \gg 3$, and therefore, the underestimation of the k_f value was first assumed as a probable reason for the misfit. The correlation of Griffin and Dranoff[21] for the adsorption of glycerol over Amberlyst beads gave a higher value of the k_f coefficient. With respect to the breakthrough point, this can be a priori defined as the time (or eluted volume) for which $C/C^0 = 0.5$. In Figure 1, it can be readily seen that this almost completely depends on the value of K, i.e., the Henry's constant for adsorption from dilute solutions. The best adjusting value was $K = 0.135$ m^3 kg^{-1}.

(12) Wakao, N.; Funazkri, T. *Chem. Eng. Sci.* **1978**, *33*, 1375.
(13) Li, P.; Xiu, G.; Rodrigues, A. E. *Chem. Eng. Sci.* **2004**, *59*, 3091.

Table 1. Description and Numerical Values of the Symbols in Equations 1−5

symbol	value	description and units
e	0.4	bed porosity, dimensionless
ϵ_p	0.5	pellet porosity, dimensionless
ρ_s	1400	solid density, Kg m^{-3}
ρ_p	700	pellet density, Kg m^{-3}
R_p	0.0002	pellet radius, m
d_t	0.008	tube diameter, m
L_t	0.25	tube length, m
U	0.0024	empty reactor velocity (ϵu), m seg^{-1}
u	0.0059	insterticial velocity, m seg^{-1}
P	875	fluid density, Kg m^{-3}
m	0.00466	fluid viscosity, Pa seg
D_m	6.0×10^{-9}	molecular diffusivity of glycerol in FAME, 25 °C, m^2 s^{-1}
D_p	3.0×10^{-9}	diffusivity of glycerol inside the pores, m^2 s^{-1}
Sc	888	$\mu/(\rho D_m)$, Schmidt number, dimensionless
Re	0.45	$u\rho D_p/\mu$, Reynolds number, dimensionless
D_L	1.31×10^{-6}	axial diffusivity, m^2 s^{-1}
Sh	8.51	$k_f D_p/D_m$, Sherwood number, dimensionless
Pe	454	UL/D_L, axial Pèclet number, dimensionless
k_f	1.28×10^{-4} [a] 2.94×10^{-4} [b] 2.0×10^{-3} [c]	film mass-transfer coefficient, m s^{-1}
Q		amount adsorbed, $g_{Gly}\ g_{ads}^{-1}$, $mol_{Gly}\ kg_{ads}^{-1}$
q^*		equilibrium amount adsorbed
q_m	0.133	saturation adsorption capacity, $g_{Gly}\ g_{ads}^{-1}$
K	0.13 [d] 1.1 [e]	Henry's constant for adsorption, m^3 kg^{-1}
K_L		Langmuir constant, dimensionless
Bi	1.93	$k_f R_p/(K\rho_p D_p)$, modified Biot number, dimensionless
C^0	0.11−0.25	feed glycerol concentration, weight %
C		concentration, mol m^{-3}
Z		axial coordinate, m
T		time, s

[a] Wakao and Funazkri correlation[12]. [b] Wilson and Geankoplis correlation[25]. [c] Griffin and Dranoff correlation[21]. [d] Fitted using the linear isotherm model. [e] Estimated with the UNIFAC algorithm.

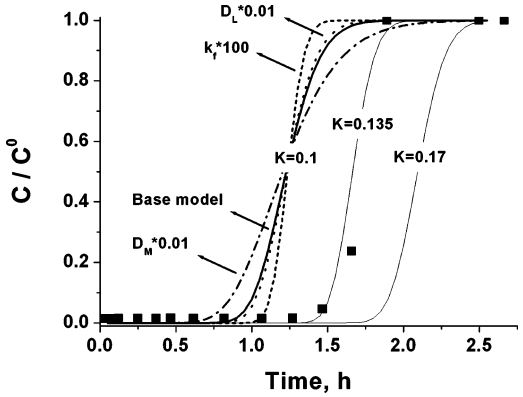

Figure 1. Comparison of an experimental breakthrough curve and the theoretical ones predicted by the linear isotherm model using different values of the Henry's constant (in m^3 kg^{-1}) for adsorption. (■) Experimental points. The conditions of the run are depicted in Table 1. (solid line) Base model.

Estimation of Adsorption Isotherm Parameters. The adjusted K value seemed to be too low, so its value was revised in order to see if this was not an artifact derived from wrong hypotheses of the model. Estimates of the K value for adsorption in the dilute concentration regime were obtained for biodiesel (FAME, fatty acid methyl esters) and for methanol (MeOH)

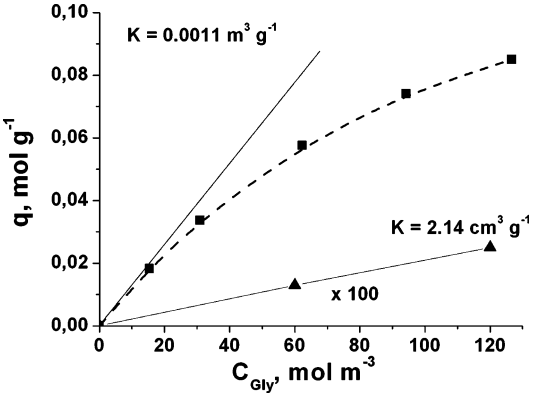

Figure 2. Adsorption isotherms for glycerol over silica in biodiesel (FAME) and methanol (MeOH) solutions as predicted by the methods of Bellot[15] and Condoret[14] using infinite dilution activity coefficients as predicted by the UNIFAC method: high dilution zone.

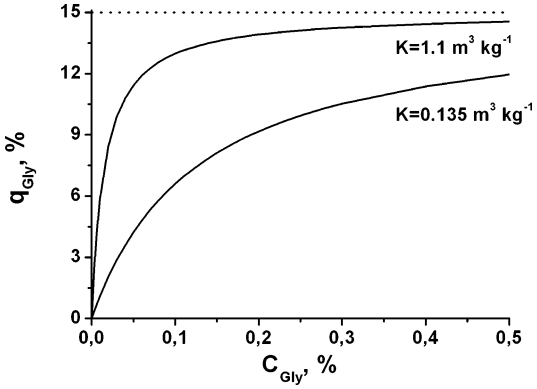

Figure 3. Langmuir isotherms constructed using the saturation value of silica for monolayer adsorption (glycerol effective surface area = 0.33 nm^2, surface area of silica = 300 m^2 g^{-1}) and the Henry's constant for adsorption as obtained with the fitting of the breakthrough curve and the linear model (K = 0.135 m^3 kg^{-1}) and the UNIFAC prediction (K = 1.1 m^3 kg^{-1}).

using the method of Bellot et al.[15] and Condoret et al.[14] The method is based on the knowledge of the curves describing the variation in the glycerol activity with respect to its concentration, established separately for each phase (solid and liquid) without considering the equilibrium between them. In the case of the activity of glycerol in the fluid phase,

$$a^{f}_{Gly} = \gamma^{f}_{Gly} \times x^{f}_{Gly} \tag{10}$$

where x^{f}_{Gly} is the mole fraction of glycerol in the fluid phase and a^{f}_{Gly} is the mole fraction based activity coefficient of glycerol in the fluid. These activity coefficients are calculated with the UNIFAC model. When considering dilute systems, as in our case, where the solvent is the dominant component, the total number of moles in the system can be approximated to that of the solvent, and the reaction volume may be estimated by the product of the molar volume of the solvent (V^f) and its number of moles. With such approximations, it is possible to rewrite eq 10 in a more appropriate way, with concentrations of components instead of mole fractions:

$$a^{f}_{Gly} = \gamma^{f}_{Gly} \times C^{f}_{Gly} \times V^{f} \tag{11}$$

With respect to the glycerol adsorption on the solid support, we have supposed there is no influence of the solvent upon the glycerol−solid interactions. The same assumption was made by Condoret et al.[14] and Bellot et al.[15] to estimate water and glycerol adsorption curves in biphasic solid−fluid systems. Finally, it is also assumed that glycerol is the only compound which can adsorb onto silica gel. At a given temperature, the activity in the solid is then given by the following:

$$a^{s}_{Gly} = k_{Gly} \times q_{Gly} \tag{12}$$

The term k_{Gly} for the silica−glycerol system has been measured and is equal to 1.5 g g^{-1} at 40 °C and normal pressure.[15] The curve of glycerol activity in the solvent as a function of its dissolved concentration is given by eq 10 if the activity coefficient γ^{f}_{Gly} is known. It was estimated here by using the UNIFAC model, as proposed elsewhere (see Figure 2).[14,15] It is then possible to relate the glycerol concentration on the solid with the concentration in the fluid phase by equating the glycerol activity values in both phases.

$$q_{Gly} = \gamma^{f}_{Gly} \times C^{f}_{Gly} \times V^{f}/k_{Gly} \tag{13}$$

This is the equation plotted in Figure 3, and Henry's constant for adsorption, K, was obtained by obtaining the slope of the approximately linear portion of the curve in the zone of infinite dilution. The value of γ^{f}_{Gly} was estimated using the original UNIFAC formulation of Fredenslund et al.[16] Ceriani and Meirelles[17] have demonstrated that the use of the original formulation predicts the VLE equilibria of fatty systems better than other ones. Recently, Negi et al.[4] have found that the UNIFAC formulation reliably predicts the activity coefficients of glycerol:methanol:methyl-oleate systems at low temperature (60 °C) though it deviates significantly from experimental data at high temperature (135 °C).

The K value predicted by the UNIFAC method is 1.1 m^3 kg^{-1} for the silica:FAME system and 0.002 m^3 kg^{-1} for the silica:MeOH system. The value 1.1 m^3 kg^{-1} is almost ten times the value produced by the adsorption model supposing a linear isotherm and no coadsorption of FAME. These two hypotheses should be revised. With respect to the phenomenon of coadsorption, the adsorption of FAME should be negligible over the adsorbent in order to make selective adsorption of glycerol feasible and to increase the efficiency of the glycerol restrainer. Nijhuis et al.[18] have indicated that in organic media the adsorption of C_8 esters over silica and Nafion resins is negligible (K = 0). In contrast, the adsorption of short chain alcohols and water displayed K values of 5 and 30 L mol^{-1}, respectively. With respect to the value of K, the studies on the adsorption of glycerol over a solid adsorbent are very scarce but some results can be found for similar polyhydroxilated molecules adsorbing from several solvents on the surface of a solid adsorbent. De Roode et al.[19] studied the adsorption of glucoside from hexanol and found that K varied between 0.1 and 0.3 m^3 kg^{-1} for several adsorbers (activated carbon, alumina, molecular sieves). Singh et al.[20] studied the adsorption of glucose on alumina from water

(14) Condoret, J. S.; Vankan, S.; Joulia, X.; Marty, A. *Chem. Eng. Sci.* **1997**, *52*, 213.
(15) Bellot, J. C.; Choisnard, L.; Castillo, E.; Marty, A. *Enz. Microb. Technol.* **2001**, *28*, 362.
(16) Fredenslund, A.; Gmehling, J.; Rasmussen, P. In *Vapor−liquid equilibria using UNIFAC*; Elsevier: Amsterdam, 1977.
(17) Ceriani, R.; Meirelles, A. J. A. *Fluid Phase Equilib.* **2004**, *215*, 227.
(18) Nijhuis, T. A.; Beers, A. E. W.; Kapteijn, F.; Moulijn, J. A. *Chem. Eng. Sci.* **2002**, *57*, 1627−1632.
(19) de Roode, B. M.; van Beek, J.; van der Padt, A.; Franssen, M. C. R.; Boom, R. M. *Enzyme Microb. Technol.* **2001**, *29*, 513.
(20) Singh, K.; Mohan, S. *J. Colloid Interface Sci.* **2004**, *270*, 21.

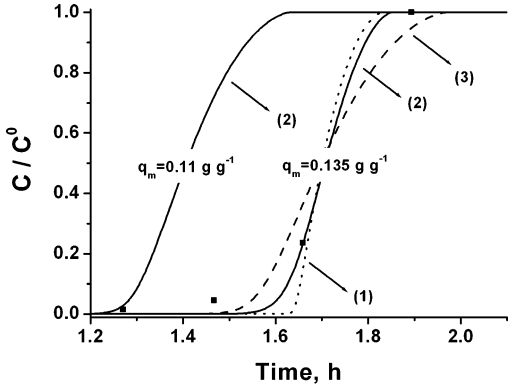

Figure 4. Weber and Chakravorti theoretical solutions for combined film and pore diffusion resistances, an irreversible square isotherm, and two values of the silica saturation capacity (q_m): (1) Griffin and Dranoff's k_f coefficient; (2) Wakao and Funazkri's k_f coefficient; (3) Wakao and Funazkri's k_f coefficient, $\tau = 2$; (■) experimental points. The conditions of the run are depicted in Table 1.

solutions. Henry's constants for adsorption can be calculated from their data as $K = 0.25$ m^3 kg^{-1}. Henry's constants for glycerol adsorption from a more organic solvent like FAME should be higher. On the other side, the UNIFAC estimated value for glycerol adsorption in the silica:MeOH system (0.00214 m^3 kg^{-1}) can be compared to the value for the adsorption of glycerol in the Amberlyst:water system (0.00072 m^3 kg^{-1}).[21] Therefore, the K values for adsorption of glycerol on silica from MeOH and FAME as predicted by the UNIFAC method seem fairly reliable. The value derived from the fitting of the breakthrough curves with the linear isotherm assumption will be revised in the following paragraphs. With respect to the obtained Henry's constant in methanol, it can be anticipated that methanol is a good solvent for performing the desorption of glycerol from silica.

A mass balance for the breakthrough experiment indicated that the total amount of glycerol adsorbed was 0.15 g_{Gly} g_{silica}^{-1}. For the 300 m^2 g^{-1} silica gel of the experiment and assuming 0.33 nm^2 as the effective surface area of glycerol,[22] the monolayer adsorption produces a maximum adsorption capacity of 0.139 g_{Gly} g_{silica}^{-1}. The total amount adsorbed in the breakthrough experiment is then very similar to the monolayer adsorption. Therefore, the experiment was performed mostly in the saturation zone of the isotherm and the linear isotherm approximation loses validity. Taking 0.15 g_{Gly} g_{silica}^{-1} as the saturation capacity ($q_m = 15\%$) and $K = 1.1$ m^3 kg^{-1} ($K = K_L q_m$), the adsorption isotherm can be rewritten in the full Langmuir form and in more useful units as follows:

$$q^*(\%) = \frac{q_m [K_L^* C(\%)]}{1 + K_L^* C(\%)} = \frac{15[64C(\%)]}{1 + 64C(\%)} \qquad (14)$$

The Henry constant predicted by the linear isotherm model ($K = 0.135$ m^3 kg^{-1}) when coupled to the q_m value of the monolayer adsorption capacity of silica produces a Langmuir isotherm that cannot explain the amount of glycerol adsorbed. Therefore, eq 14 is adopted. Both isotherms are plotted in Figure 4. In the range of glycerol concentrations of the feed (0.2−0.4%), the Langmuir isotherm can be assumed to approach the shape of a square isotherm ($q^* = q_m$); this approximation is used to analyze the breakthrough curves in the next paragraphs.

(21) Griffin, R. P.; Dranoff, J. S. *AIChE J.* **1963**, *9*, 283.
(22) Quirk, J. P.; Murray, R. S. *Soil Sci. Soc. Am. J.* **1999**, *63*, 839.

Approximate Solution for Square Isotherm. The high affinity of silica for glycerol can be taken into account by using a square isotherm and a shrinking-core model rather than a model with a variable local concentration of glycerol. The model can be further simplified by considering than one of the two acting mass-transfer resistances is much higher than the other. If the film resistance is calculated with the correlation of Griffin and Dranoff[21] and if the molecular diffusivity predicted by the Wilke−Chang equation is adopted, the average resistances can be calculated as follows:

$$1/k_f = 1000 \text{ s m}^{-1} \qquad (15)$$

$$R_p/4\epsilon_p D_M = 0.0002 \text{ m}/(4.0 \times 0.5 \times 6.0 \times 10^{-9} \text{ m}^2 \text{ s}^{-1}) = 8333 \text{ s m}^{-1} \qquad (16)$$

There is not a big difference between the two resistances, but the diffusion resistance is higher even at the small R_p value of the experiment ($R_p = 0.2$ mm). At higher R_p values such as those encountered in industrial packed bed adsorbers (e.g., R_p = 1/16−1/8 in.), the difference between the mass-transfer resistances would be much higher and pore diffusion would dominate as rate determining step. For a shrinking-core model dominated by pore diffusion, the local mass transfer is given by the following:

$$4\pi q_m \rho_p r_c^2 (1/R_p - 1/r_c) \frac{\partial r_c}{\partial t} = 4\pi D_M C_{Gly} \qquad (17)$$

The term r_c would be a function of the axial coordinate z and of time. Now, the model would include eqs 1, 2, 5, 13, and 16. A full solution can be obtained by numerical methods, but analytical solutions are also available for some approximate models. For the constant pattern regime, the relevant expressions for the adsorption influenced both by pore diffusion and film mass-transfer limitations have been given by Weber and Chakravorti:[23]

$$\theta - N_p = \frac{15}{\sqrt{3}} \tan^{-1}\left[\frac{2(1-Q)^{1/3}}{\sqrt{3}} + 1\right] - \frac{15}{2} \ln[1 + (1-Q)^{1/3} + (1-Q)^{2/3}] + 2.5 - \frac{5\pi}{2\sqrt{3}} + \left(\frac{N_p}{N_f}\right) \ln(Q+1) \qquad (18)$$

$$\theta = \left[\frac{15\epsilon D_p}{R_p^2}\right]\left[\frac{C^0}{q_s}\right](t - z/v) \qquad (19)$$

$$N_p = \left[\frac{15\epsilon D_p}{R_p^2}\right]\left[\frac{1-\epsilon}{\epsilon}\right]\left(\frac{z}{v}\right) \qquad (20)$$

$$N_f = k_f\left[\frac{1-\epsilon}{\epsilon}\right]\left(\frac{3z}{vR_p}\right) \qquad (21)$$

$$Q = \frac{q}{q_s} = \frac{C}{C^0} \qquad (22)$$

The constant pattern condition is fulfilled in most of the span of the breakthrough experiments ($\theta > 5/2 + N_p/N_f$) except in the initial region when the pattern is developing. The simplified

(23) Weber, T. W.; Chakravorti, R. K. *AIChE J.* **1974**, *20*, 228.

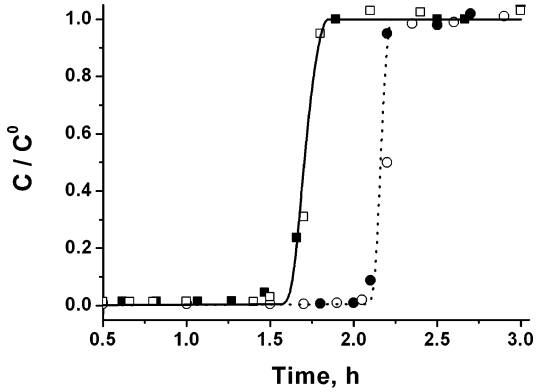

Figure 5. Influence of the regeneration with methanol: (■) first run, fresh adsorbent, $C^0 = 0.11\%$, and $U = 14.4$ cm min^{-1}; (▲) second run, adsorbent regenerated by eluting 4 bed volumes with methanol and then drying; (□, △) idem with $C^0 = 0.25\%$ and $U = 5$ cm min^{-1}.

expression for dominant pore diffusion can be obtained by setting $(N_p/N_f) \approx 0$.

The predicted results of Weber and Chakravorti's model are plotted in Figure 4 along with the experimental results for one breakthrough curve. It must be recalled that in the case of the linear isotherm model (Figure 1) the experimental curve was better fitted by assuming low values of the mass-transfer resistances. In contrast in the case of the square isotherm model, the common Wakao and Funazkri correlations gave good results and the results can be slightly improved by assuming a tortuosity factor $\tau = 2$ to further reduce the effective diffusivity.[24] The Wakao and Funazkri correlations were therefore adopted for all simulated breakthrough curves. It can also be seen in Figure 4 that now the adsorption saturation capacity q_m is the parameter primarily establishing the breakthrough point.

Regeneration of the silica bed was attempted by eluting a methanol volume equal to 4 bed volumes with an inlet velocity of 14.4 cm^{-1} approximately and then drying with a flow of nitrogen. With less than 1 bed volume of methanol, almost all the retained glycerol was desorbed as determined by visual inspection. With 4 bed volumes of eluted methanol, it was considered that desorption was complete. When nitrogen was allowed to flow, a fairly big decrease of the temperature of the silica bed was detected. This temperature decrease was attributed to the evaporation of adsorbed methanol. For a monolayer of methanol adsorbed, its evaporation demands 150 J per gram of silica. This amount of heat must be provided by the carrier gas in order to maintain the temperature of the silica bed. After the desorption, the adsorption experiment was repeated. These results are presented in Figure 5 for two experiments with different space velocities. It can be seen that the regeneration is seemingly complete. In order to confirm that all glycerol was eliminated during the flushing of the column with methanol, temperature programmed oxidation (TPO) tests were also performed. The results are plotted in Figure 6. The TPO trace of a silica sample intentionally filled with glycerol (0.56 g_{gly} g_{silica}^{-1}, four monolayers) has two main peaks, a sharp one located at 245 °C and another broad one at 350 °C. The areas of the TPO traces of the fresh silica or of the regenerated silica are 1000 times smaller, indicating that the amount of glycerol retained after regeneration is negligible.

Additional results were predicted by using the Weber and Chakravorti model for industrial scale silica beds for glycerol adsorption. These results are plotted in Figures 7−9. Parameters

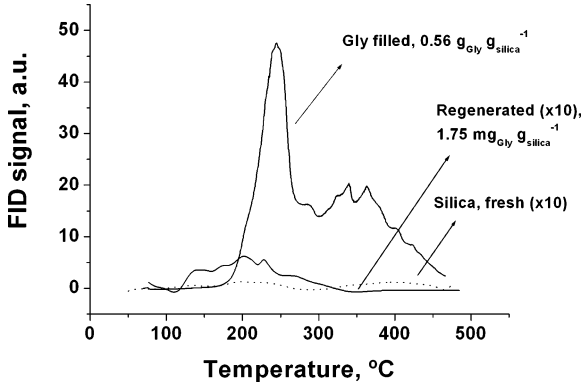

Figure 6. Temperature programmed oxidation of fresh, glycerol-filled, and regenerated silica. The adsorbent was regenerated by eluting 4 bed volumes with methanol and then drying in nitrogen.

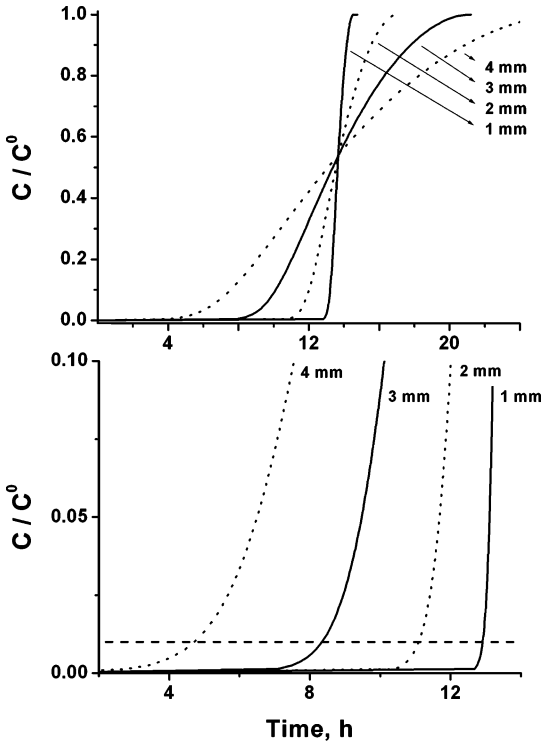

Figure 7. Breakthrough curves simulated with Weber and Chakravorti's model: influence of the pellet diameter. Below is shown an enlarged portion of the plot to visualize the breakthrough point and the breakthrough limit $C/C^0 = 0.01$. Bed height = 2 m; $U = 14.4$ cm min^{-1}.

were varied in order to see the influence of the pellet diameter, the inlet velocity, and the Gly concentration of the feed.

The influence of the pellet diameter can be visualized in Figure 7 at two concentration scales. For a small diameter (1 mm), the saturation and breakthrough points practically coincide and the traveling mass-transfer front is almost a concentration step. For higher diameters, the increase in the time of diffusion of glycerol inside the particles produces a stretching of the mass front and a more typical sigmoidal curve appears. The breakthrough point in our case should be defined as $C/C^0 = 0.01$. For common C^0 values (0.1−0.25% glycerol in the feed), lowering the glycerol content to the quality standards for biodiesel (0.002%) demands that C/C^0 at the outlet is equal or lower than 1% of the value of the feed. The results indicate that for a 3 mm pellet diameter ($\approx 1/8$ in.) the breakthrough time is reduced from 13 to 8 h and that for a 4 mm pellet diameter this value is further reduced to 4.5, i.e., almost one-third of the

(24) Wakao, N.; Smith, J. *Chem. Eng. Sci.* **1962**, *17*, 825.
(25) Wilson, K.; Geankoplis, T. *Ind. Eng. Chem. Fundam.* **1966**, *5*, 9.

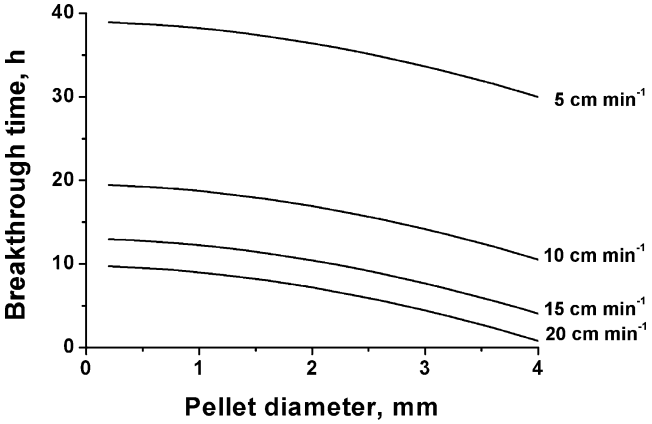

Figure 8. Simulated breakthrough curves: influence of the pellet diameter on the breakthrough time. Bed height = 2 m; breakthrough time at C/C0 = 0.01.

saturation time. In can be inferred that the pellet diameter has a strong influence on the processing capacity of the silica bed. Small diameters though convenient from this point of view are not practical, and the pellet diameter is usually in the range 3−6 mm in industrial adsorbers for process-related reasons such as reduction of the pressure drop or decrease of the adsorber attrition.

The combined influence of pellet diameter and inlet velocity on the breakthrough time is depicted in Figure 8. Similar trends are clearly distinguished. The breakthrough time seems to depend on $D_p^{1/n}$ ($n > 0$) and also on $U^{1/n}$ ($n > 0$). This means that longer breakthrough times are obtained at smaller pellet diameters and smaller feed velocities. However, this does not directly tell us whether the processing capacity per unit kilogram of silica is higher under these conditions. Such information is displayed in Figure 9, taking different values of the concentration of glycerol in the feed and a fixed value of the pellet diameter (3 mm). When the feed velocity tends to zero, the bed capacity tends to be equal to q_m and this value decreases almost linearly when increasing the velocity. For a typical solid−liquid velocity of 5 cm min^{-1}, the analysis of the capacity as a function of the glycerol feed concentration indicates that the capacity decreases at higher glycerol concentrations but that the silica bed is used more efficiently at higher glycerol concentrations. This is due to the fact that for diluted feeds the relative importance of the mass-transfer zone (sigmoidal region) with respect to the total length of the breakthrough curve is higher.

Conclusions

Fresh beds of silica gel can effectively reduce the glycerol content of biodiesel to contents lower than that specified in the ASTM standard. The breakthrough time is defined as that one

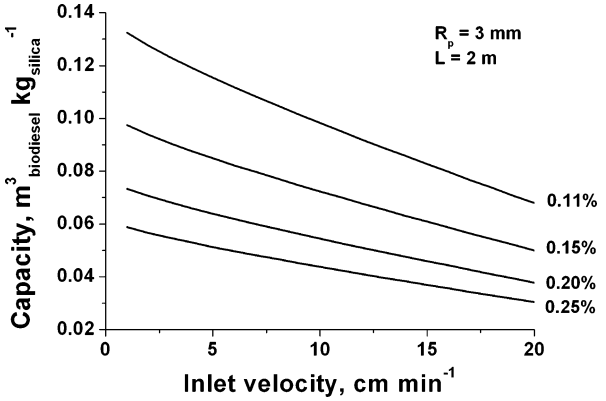

Figure 9. Simulated breakthrough curves: influence of inlet velocity on the processing capacity. Pellet diameter = 3 mm; bed height = 2 m.

for which the ASTM quality limit was reached. For a feed velocity of 14 cm min^{-1}, breakthrough times in excess of 1 h were obtained. Regeneration with methanol proved to be an effective means of regenerating the bed. The adsorption capacity of a silica bed flushed with 4 bed volumes of pure methanol and dried with nitrogen for 1 h is practically the same as that of a fresh silica bed. Thus, a cyclic operation of a silica bed for glycerol removal was found to be feasible and simple.

It was found that the Henry's constant for adsorption could be reliably estimated when the activity of the solute (glycerol) on the solid was known and the activity of the solute in the solvent at infinite dilution was calculated using the UNIFAC method (K_{Henry} = 1.1 m^3 kg^{-1}). Experimental breakthrough curves indicated that the saturation capacity was 0.135−0.15 g g^{-1}. This is practically the value for monolayer adsorption.

The breakthrough curves at the flow conditions of the test (small particle diameter, low space velocities) could be accurately predicted by assuming a square isotherm with q_m = 0.135 g g^{-1} and a shrinking-core model with both pore diffusion and film mass-transfer resistances. The effect of axial diffusion was found to be negligible. Intrapellet diffusion and mass transfer through the film did not affect the breakthrough time very much for small pellet diameters (<1 mm) but were quite important for pellet diameters typical of industrial adsorbers (>3 mm). For these pellet sizes and for typical glycerol feed concentrations (0.1−0.25%) and velocities (5−10 cm min^{-1}), the bed breakthrough time is achieved in about one-half to one-third of the time of bed saturation for no mass-transfer resistance.

Acknowledgment. This work was performed with the financial support of the Universidad Nacional del Litoral (Santa Fe, Argentina) and CONICET through the CAI+D 2002-20-146 and PICT 2004-26144 grants.

EF060362D